NJC

ROYAL SOCIETY OF CHEMISTRY

PAPER

View Article Online
View Journal | View Issue



Cite this: *New J. Chem.*, 2023, **47**, 2520

# β and γ-Cyclodextrin dimers: design, characterization and *in silico* studies to explore the cooperative effect of the cavities†

Luana La Piana,‡[a] Livia Basile,‡[a] Chiara Ragusa,[a] Danilo Milardi,[b] Valeria M. V. Zito[b] and Graziella Vecchio*[a]

Cyclodextrins can encapsulate various molecules and have exciting applications in supramolecular, pharmaceutical, material, food and environmental chemistry. Typically, the encapsulation into the cyclodextrin cavity confers to the guest improved solubility, stability, bioavailability and organoleptic properties. In recent years, cyclodextrin multi-cavity systems have also been studied to encapsulate biomolecules or drugs. This context has inspired us to synthesize and characterize two new β and γ-cyclodextrin dimers and compare their complexation behavior. The two cavities in the same molecule significantly improve the stability of inclusion complexes. Particularly we investigated cholic acid, cholesterol and doxorubicin as guests. The extent of binding between a guest molecule and β and γ-cyclodextrin dimers was established by molecular docking. Cholic acid at physiological pH was chosen as a water-soluble cholesterol analog for the investigation in water by isothermal calorimetry. We found that dimers can include cholate species, cholesterol and doxorubicin better than native cyclodextrins, and the cyclodextrin type tunes the stability of inclusion complexes.

Received 20th September 2022,
Accepted 23rd December 2022

DOI: 10.1039/d2nj04649k

rsc.li/njc



## Introduction

Cyclodextrins (CyDs) are cyclic glucose oligosaccharides α(1 → 4) linked. CyDs have a truncated cone shape with a predominantly hydrophobic cavity and the OH groups are placed on exterior surfaces.[1,2] The number of glucose units (six αCyD, seven βCyD and eight γCyD) determines the features of the cavity and its size. CyDs can encapsulate various molecules for these unique features and have found exciting applications in supramolecular, pharmaceutical, material, food and environmental chemistry.[1–4]

Typically, the encapsulation into the CyD cavity confers to the guest improved solubility, stability, bioavailability and organoleptic properties.[3,5] A variety of drugs or biomolecules can be included in CyD with different stoichiometries of inclusion complexes.[6–9]

The chemical modification of CyDs has extended the range of applications of their chemistry.[10–12]

The addition of functional groups or lipophilic chains at CyD rims can also modulate the inclusion abilities of CyD cavities.[13–15] Many derivatives have been synthesized to improve the potential of CyDs. Thus, several CyD-based conjugates with amines, biomolecules, and drugs have been designed over the years.[16–18]

CyD derivatives are also used in clinical as therapeutic nanocavities, such as sugammadex and hydroxypropyl β-cyclodextrin (HPβCyD). Sugammadex has been designed to include rocuronium and reverse its effect in humans.[19] Furthermore, HPβCyD has been approved as an orphan drug for Niemann Pick Type C and focal segmental glomerulosclerosis.[20] The ability of HPCyD to include molecules has also been exploited to disrupt virus membranes and act as an antiviral therapeutics.[21]

In recent years, CyD multi-cavity systems have also been studied to improve drug inclusion.[22–25] CyD dimers have also been synthesized with linkers with different lengths and rigidity.[26–32] The length, flexibility, and structure of the linker connecting the two CyDs may considerably affect the thermodynamic parameters of inclusion phenomena and determine the host–guest binding modes.[32]

In this context, the design and the studies of nanocapsules based on CyDs with high and selective complexation ability are of interest.

We synthesized new β- and γ-CyD dimers linked *via* a glutamic acid linker (Fig. 1). The linker has an amino group

[a] *Dipartimento di Scienze Chimiche, Università degli studi di Catania, V.le A.Doria 6, 95125, Catania, Italy. E-mail: gr.vecchio@unict.it*
[b] *Istituto di Cristallografia, Consiglio Nazionale delle Ricerche, Via P. Gaifami 18, 95126, Catania, Italy*

† Electronic supplementary information (ESI) available: NMR spectra. See DOI: https://doi.org/10.1039/d2nj04649k

‡ These authors equally contributed.

 

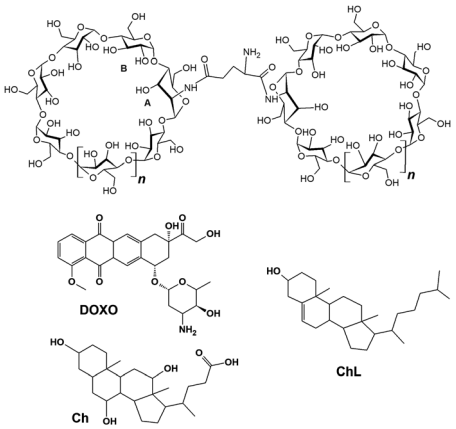


Fig. 1 Cyclodextrin dimers ($n$ = 1 βCyD2Glu, $n$ = 2 γCyD2Glu) and guests investigated.

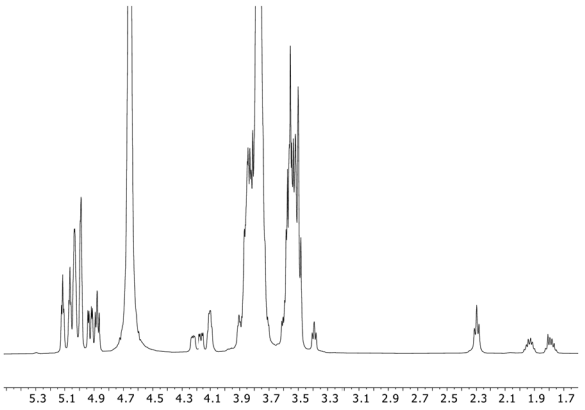


Fig. 2 $^1$H NMR spectrum of γCyD2Glu ($D_2O$, 500 MHz).

that can be protonated or permits further modification of the systems. We explored the advantage of CyD dimers and the role of CyD type (β or γ) in including biomolecules (cholic acid and cholesterol) or drugs (doxorubicin). Cholesterol, cholic acid and doxorubicin are model guests widely studied. Their studies into the new derivatives can improve the potential of CyDs as nanocapsules. The inclusion capability of the dimers was investigated through a multi techniques approach by molecular docking, NMR spectroscopy and isothermal titration calorimetry (ITC) experiments.

We further investigate these aspects by considering new β and γ-CyD dimers. ITC has been used to provide the binding constant, $\Delta H^\circ$, $\Delta S^\circ$ for inclusion complexes of dimers with cholic acid at physiological pH (cholate species) and data were compared with those obtained for native β and γCyD.

## Results and discussion

### Synthetic aspects

The CyD dimers were synthesized starting from γCyDNH$_2$ or βCyDNH$_2$ and Boc–Glu–OH (Fig. S1, ESI†). Amino-CyDs contain an altrose unit due to the preparation methods.

NMR spectra characterized the new dimers. In the $^1$H NMR spectra, the signal of the CyD units and the linker can be identified. The functionalization with the asymmetric linker makes the two CyDs different, particularly in the H-1 region.

In the spectra of γCyD2Glu (Fig. 2), the H-1s spread in more groups and the signals of altrose rings are at 4.88 and 4.87 ppm. The other protons of the functionalized altrose rings (A) are also identified with COSY and TOCSY spectra in the range of 3.65–3.45 ppm. In the H-1 region, the glucose rings adjacent to A rings are also clearly identified by ROESY spectra at 4.94 and 4.92 ppm.

Similar behavior was found for βCyD2Glu. In the spectra, H-1 signals of altrose units are at 4.86 and 4.85 ppm.

### Inclusion complexes

**Docking analysis.** Docking studies were performed to analyze the inclusion mechanism of guest molecules by β- and γ-CyD2Glu and evaluate the binding affinities.

Given the amphiphilic nature of CyD, the binding affinity of cholesterol and/or similar molecules results from different factors like hydrophobic interactions, van der Waals forces, and complementarity of the shape and size between host and guest molecules.[33] Thanks to the ability to fully embed cholesterol and/or similar molecules, CyD dimers can be more efficient in term of molecular docking in comparison to their native CyD[34] (Table 1).

In this study, the dimer was considered in the form of a single closed conformation as the result of hydrogen bonds between the secondary hydroxyl groups, which affects its flexibility.[35]

Overall, the binding affinity (Table 1) calculated by docking calculations indicates that CyD dimers form more stable inclusion complexes with a higher degree of binding than native cyclodextrins (Fig. S10, ESI†). Fig. 3 shows the best docking poses of ligands, with each cavity represented as host a and host b according to the orientation of the linker. Differences in the pattern of interactions were found after the examination of docking output. Analysis of Ch binding mode reveals that the guest molecule is approximately positioned in the middle of the β dimer, where the binding site was defined (Fig. 3).

The β-dimer roughly engulfs the ligand with its carboxylate group protruding from the narrow rim of the host **a** and the hydroxyl group of the A ring in the ligand interacting by an H bond with the glycosidic oxygens of the host **b**. Another H bond between the oxygen atom of the carboxylate group and the primary hydroxyl group at the narrow rim of host **a** contributes to stabilizing the complex. A different interaction pattern was found when cholate was docked inside the γ-dimer binding site. In particular, the ligand was accommodated at the dimer interspace with the OH of ring A and its carboxylate group forming H bonds with the glycosidic oxygen of the host **a** and

Table 1 Docking score (Kcal mol$^{-1}$) for native CyDs and CyD dimers

| Ligand | βCyD | γCyD | βCyD2Glu | γCyD2Glu |
|---|---|---|---|---|
| Cholesterol | −5.5 | −5.6 | −8.4 | −7.2 |
| Cholate | −6.6 | −6.6 | −8.6 | −8.1 |
| Doxorubicin | −7.7 | −7.2 | −6.2 | −9.3 |

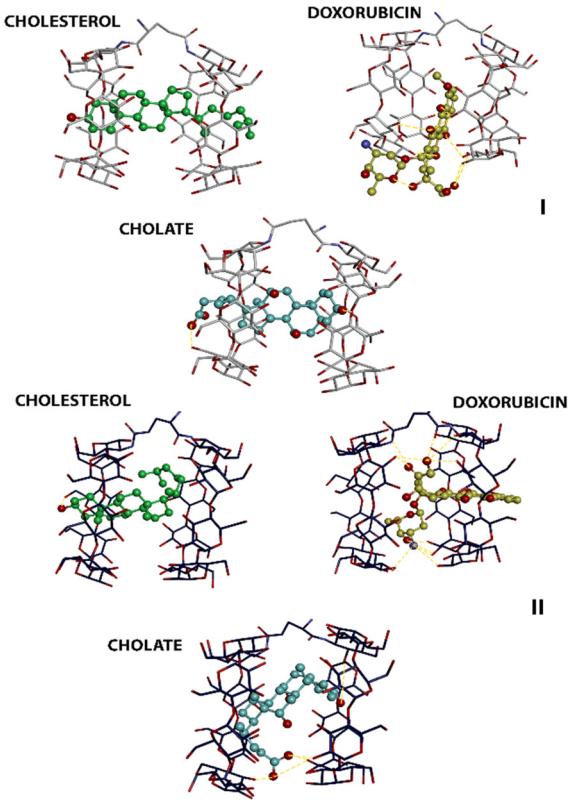


Fig. 3 Docking pose of cholate (blue), cholesterol (green) and doxorubicin (–$NH_3^+$ in the daunosamide group, yellow) into the cavity of β- (I) and γ-CyD (II) dimers. H bond interactions are depicted by yellow dotted lines.

with hydroxyl groups of both wider rims. As for docking of cholesterol with β-CyD dimer, the ligand is stably accommodated inside the βCyD dimeric cavity.[30] In this structure, the hydroxyl group puts forward the narrow rim of the host **b**, which tightly embraces ring A of the sterol group. Meanwhile, the aliphatic tail is enclosed in the hydrophobic cavity of the host **a**. A different trend was observed in the case of docking of cholesterol with γCyD dimer mainly due to a different orientation of the aliphatic tail of the ligand that is located at the dimer interspace and folded on the sterol group. Moreover, the hydroxyl group of ligand forms an H bond with the hydroxyl group of the narrow rim of the host **a**. Docking scores obtained by simulating doxorubicin demonstrate different binding affinity between β- and γ-dimers. When the drug is in the complex with β-dimer, it was not encapsulated but it was constrained in a ''sandwich'' mode in the interspace of the β-dimer with the sugar moiety laying outside both cavities. Hydroxyl groups on the wide rims of dimer form preferably H bond interactions with the conjugated ring system of the drug, especially with rings B and C, and the acetyl moiety of the drug. Best docking pose of doxorubicin with γ-dimer shows that the hydroxyanthraquinone core is enclosed in the host **b** macrocycle cavity with the OH of the ring B forming an H bond with the glycosidic oxygen, whereas the daunosamine group is located at the interface of the dimer interacting by H bonds with the hydroxyl groups of both wide rims. Interestingly, the inclusion complex gains stability from H bonds between the glutamic acid linker and the hydroxy acetyl moiety of the drug. Moreover, a tight network of H bonds was found between the hydroxy acetyl moiety and the hydroxyl groups of wide rims of the dimer. Overall, these docking results suggest a more extended inclusion of ligands by dimers in comparison to native CyD that should guarantee higher stability of complexes.

**NMR spectroscopy.** We investigated the inclusion of Ch or DOXO into CyD dimers by NMR.

Ch was used as a cholesterol analog because the inclusion complexes with cholesterol are not soluble enough in the water for the NMR spectroscopy and ITC study. On the other hand, organic solvents disfavor guest inclusion. The NMR spectra of Ch with CyD2Glu dimers are reported in Fig. 4 and Fig. S10–S15 (ESI†).

$^1$H NMR spectra of Ch/γCyD2Glu showed a shift of the CyD proton resonances evident in the H-1 region. Furthermore, Ch protons in the presence of CyD are shifted compared to the free Ch. Ch H-7 proton is downfield shifted and H-12 is upfield shifted. This trend is also well evident in the 2.2–0.6 ppm region. This behavior strongly suggests the interaction of Ch with CyDs.

ROESY spectra of Ch/γCyD2Glu (1 : 1 molar ratio, Fig. S12–S14, ESI†) showed the cross-peaks between the protons of the steroid ring and H-3, H-5 region of CyD moiety. Ch methyl groups showed intense cross-peaks with the CyD protons.

As for Ch/βCyD2Glu, Ch and CyD protons are shifted compared to the free components. Ch H-7, H-12, H-3, H-18, H-19 and H-21 are downfield shifted compared to the free Ch (Fig. S14–S18, ESI†). This trend is also well evident for other protons of the steroid ring. In the ROESY spectra, cross-peaks between Ch and CyD H-3, H-5 suggest the inclusion of Ch into CyD cavities.

ROESY spectra showed stronger correlation peaks between CyD H-3, H-5 and Ch protons than γCyD2Glu. This behavior supports the docking studies suggesting that the sterol group is located at the dimer interspace.

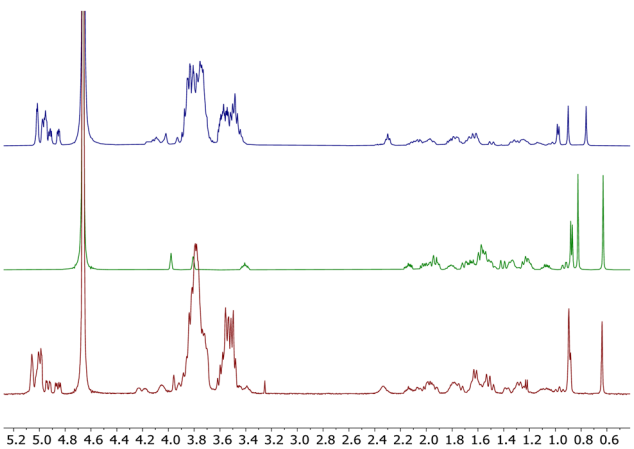


Fig. 4 $^1$H NMR spectrum of Ch/CyD2Glu 1 : 1 molar ratio (500 MHz, $D_2O$): Ch/βCyD2Glu (top), Ch alone (middle), Ch/γCyD2Glu (bottom).

 

$^1$H NMR spectra were also carried out in the presence of an excess of Ch to explore the possible inclusion of two Ch molecules.

Inclusion complexes with dimers and DOXO were also investigated with NMR (Fig. S19–S21, ESI†). When DOXO was added to γCyD2Glu signals of the anthracycline protons were broad in the aromatic region compared to free DOXO and downfield shifted, mainly H-1 and Hs-10. The H-1 region also shows some modifications and the downshift of H-7 of the anthracycline ring. This data is in keeping with the docking study that suggests a network of H bonds involving the anthracycline A ring and secondary OH group.

Although the signals of DOXO protons overlap with those of CyD, ROESY spectra suggest the correlation of aromatic protons with H-3, H-5 region of γCyD (Fig. S21, ESI†).

As for βCyD2Glu, signals of the aromatic protons are also broad and H-4 is slightly downfield shifted compared to free DOXO. In the ROESY spectra, no correlation with the H-3 and H-5 region of CyD are present. This data may support docking studies that suggest a ''sandwich'' disposition of the anthracycline ring in βCyD2Glu.

**ITC experiments.** Due to the low solubility of DOXO and cholesterol at physiological pH, ITC experiments were performed only to investigate cholate/CyD and CyD2Glu systems.

We determined the values of $K_D$, $\Delta H$ and $\Delta S$ for the inclusion of cholate within βCyD, γCyD and their dimer derivatives. Results of ITC cholate/βCyD and cholate/γCyD experiments are shown in Fig. 5. The first points were not considered in the data analysis due to the passive diffusion of the titrant solution into the reaction cell during equilibration at the tip of the syringe. The gross heats of the reaction were corrected for the cholate-buffer dilution effects to obtain the heat rate (Fig. 5 top panels). Normalized heat was obtained by integrating the heat rates and then plotted as a function of the cholate/CyD molar ratio. Data analysis of ITC experiments is obtained under the assumption of a 1 : 1 stoichiometry ($n$ = 1) model for both β and γCyD (see Table 2). The positive $\Delta S$ values indicate that the inclusion of cholate in both β and γCyD is thermodynamically driven by the displacement of water molecules from the hydrophobic CyD cavity. Moreover, entropy changes relative to cholate binding to γCyD are higher than βCyD, following that the inclusion into a larger CyD cavity is associated with higher $\Delta S$ values consequent to the displacement of more water molecules to the solvent (hydrophobic effect).[36] Fig. 6 reports calorimetric titrations of β- and γCyD2Glu. Initially, any attempt to get the thermodynamic parameters by fitting the entire calorimetric titration either with a guest/CyD 1 : 1 or 2 : 1 model failed for both βCyD2Glu and γCyD2Glu. However, we observed that ITC traces for both cyclodextrin dimers might be conveniently fitted with a 1 : 1 and a 2 : 1 guest/host model at low (from 0 to 2) and high (from 3 to 5) molar ratios, respectively (see Table 2). According to the thermodynamic parameters obtained, we can infer that at low molar ratios, both CyD dimers may accommodate one Ch molecule with a $K_D$ lower than that determined for the corresponding CyD. However, entropic factors are much more preponderant for this binding event, suggesting that assistance of the second cavity to the accommodation of the guest may occur in accordance with molecular docking (see Fig. 3). At higher molar ratios, CyD2Glu systems may include two Ch molecules with $K_D$ in the range of those observed for CyD. In this second step, the entropic contribution, albeit preponderant, is lower than in the first step, suggesting an inclusion process more similar to the native CyD. These observations are consistent with a mechanism where, at lower guest/dimer molar ratios, the guest bridges the two cavities of the dimer (1 : 1 cooperative binding mode). By contrast, at higher guest/dimer molar ratios, each cavity of the dimer interacts with one guest molecule (two-sites binding mode). The lower entropic contribution associated with the two sites binding mode may be ascribed to the displacement of fewer water molecules upon inclusion.

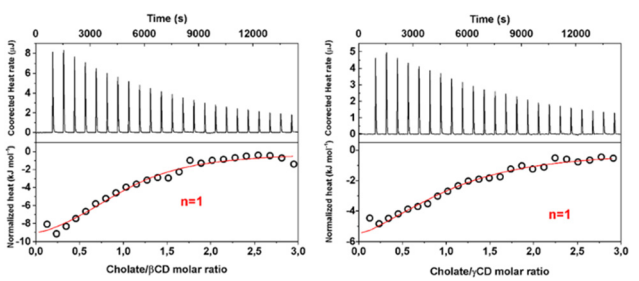


Fig. 5 ITC thermograms of the titration of cholate with βCyD (left) and γCyD (right). To calculate the thermodynamic inclusion parameters the corrected heat rates (top) were analyzed by a 1 : 1 model (bottom).

## Experimental

### Materials and reagents

Commercially available reagents were used directly unless otherwise noted. Boc–Glu–OH (*N*-*tert*-butoxycarbonyl-L-glutamic acid), 3A-amino-3A-deoxy-2A(S),3A(R)-β-Cyclodextrin ($\beta$CyDNH$_2$) and 3A-amino-3A-deoxy-2A(S),3A(R)-γ-Cyclodextrin ($\gamma$CyDNH$_2$), cholesterol, sodium cholate and doxorubicin were purchased from TCI. Thin Layer Chromatography (TLC) was carried out on silica gel plates (Merck 60-F254). Carbohydrate derivatives were detected on TLC by UV light and anisaldehyde test.

### NMR spectroscopy

$^1$H and $^{13}$C NMR spectra were recorded at 27 °C with a Varian UNITY PLUS-500 spectrometer at 499.9 and 125.7 MHz, respectively. The NMR spectra were obtained using standard pulse programs from the Varian library. 2D experiments (COSY, TOCSY, gHSQCAD, gHMBC, ROESY) were acquired using 1k data points, 256 increments and a relaxation delay of 1.2 s. The sugar units in CyD are labeled A–G or A–H counter-clockwise starting from the modified ring (A), as viewed from the secondary rim. Two CyDs in dimers are labeled X (γ COOH) and Y.

Steroid rings of Ch are labeled A to D, and atoms are numbered 1 to 27, according to IUPAC-recommended nomenclature (Fig. S9, ESI†). DOXO is labeled as reported in Fig. S9 (ESI†).

Table 2 Cholate/CyD and CyD2Glu complexation parameters obtained by fitting calorimetric titrations by a 1 : 1 ($n$ = 1) and 2 : 1 ($n$ = 2) stoichiometry. The statistics function of the Nanoanalyze software was used to estimate the uncertainties of the model parameters (confidence level = 95%)

| | | | βCyD2Glu | | γCyD2Glu | |
|---|---|---|---|---|---|---|
| | βCyD | γCyD | 1 step | 2 step | 1 step | 2 step |
| $n$ | 1 | 1 | 1 | 2 | 1 | 2 |
| $K_D$ (M) | $(1.7 \pm 0.4) \times 10^{-4}$ | $(1.4 \pm 0.3) \times 10^{-4}$ | $(5.9 \pm 4.7) \times 10^{-5}$ | $(4.0 \pm 1.1) \times 10^{-4}$ | $(4.7 \pm 4.8) \times 10^{-5}$ | $(2.4 \pm 1.5) \times 10^{-4}$ |
| $-\Delta H$ (kJ mol$^{-1}$) | 17.0 ± 1.4 | 8.1 ± 0.5 | 3.0 ± 2.9 | 5.3 ± 0.5 | 1.27 ± 1.1 | 1.10 ± 0.2 |
| $\Delta S$ (J K$^{-1}$ mol$^{-1}$) | 15.30 | 46.47 | 70.78 | 47.26 | 78.50 | 65.30 |

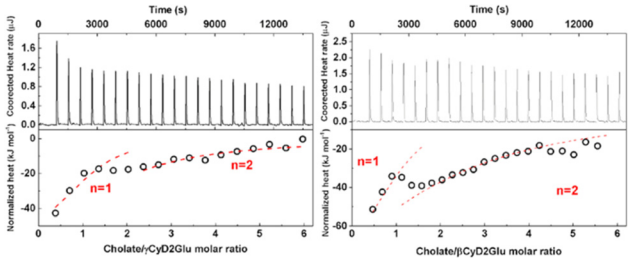


Fig. 6 ITC thermograms of the titration of cholate with βCyD2Glu (right) and γCyD2Glu (left). To calculate the thermodynamic inclusion parameters the corrected heat rates (Top) were analyzed by a 1 : 1 or a 2 : 1 guest/host model (bottom).

## ITC titrations

Calorimetric measurements were recorded at 25 °C using a Nano-ITC calorimeter (TA Instruments). All solutions were carefully degassed by vigorous stirring under vacuum. Calorimetric measurements were conducted in 10 mM phosphate buffer (pH 7.4) by titrating a 3.0–4.6 mM cholate solution into a 0.15–0.36 mM CyD solution. The reaction mixture was stirred in the sample cell at 250 rpm during the experiment. The calorimeter was routinely calibrated by titrating a 1.0 mM HCl solution into a 30 mM TRIS buffer, as previously reported.[37] In a typical guest/CyD binding experiment, the cholate solution was injected into a 950 mL sample cell containing CyD in 25 aliquots of 9.98 μL (except the first injection, which was 2 μL) with a time interval between injections of 600 s. To obtain the cholate dilution heat while maintaining pH and phosphate concentrations, the reaction cell was only filled with the buffer solution in the blank experiments, while the syringe was filled with the corresponding buffered cholate solution. The gross heat evolved/absorbed in the reaction was analyzed using the NanoAnalyze software (TA Instruments, New Castle, USA).

## 3A-Deoxy-3A-(*N*-butoxycarbonyl)-2A(S),3A(S)-β-cyclodextrin (βCyD2Glu)

EDC (1-ethyl-3-(3-dimethylaminopropyl)carbodiimide) (17 mg, 0.088 mmol) and HOBt (1-hydroxybenzotriazole) (12 mg, 0.088 mmol) were added to Boc–Glu–OH (10.9 mg, 0.044 mmol) in dry DMF. After 10 min, $\beta CyDNH_2$ (100 mg, 0.088 mmol) and Triethylamine (0012 mL, 0.088 mmol) was added to the DMF solution. The reaction mixture was stirred at room temperature for 24 h under stirring. The reaction mixture was added to water and purified by dialysis (Float-A-LyZer G2, MWCO 1000). The solvent was evaporated to dryness *in vacuo*. The product βCyD2GluBoc was added to $CF_3COOH$ under stirring for 6 h to remove the Boc group. The solvent was evaporated and the reaction mixture was purified by Sephadex CM C-25 column ($NH_4^+$ form) using a linear gradient $H_2O$–$NH_4HCO_3$ (0 → 0.2 M) as the eluent. Yield: 42%.

### ESI MS $m/z$ 2379.2 $[M + H]^+$

$^1$H NMR (500 MHz, $D_2O$) $\delta$ (ppm): 5.03 (m, 4H, H-1 of CyD), 4.97 (m, 4H, H-1 of CyD), 4.94 (m, 3H, H-1 of CyD), 4.91 (d, 1H, $J$ = 4.1 Hz, H-1G of CyD), 4.87 (m, 2H, H-1AX, H-1AY of CyD), 4.20 (m, 1H, H-3A X CyD), 4.16 (m, 3H, H-3AY and H-5A of CyD), 3.65 y–3.45 (m, 64 H, H-2AX, H-2AY, H-4A, H-3, H-5, H-6 of CyD), 3.62–3.45 (m, 24 H, H-2, H-4 of CyD), 3.43 (t, 1H, $J$ = 6.5 Hz, H-α of Glu), 2.29 (t, 2H, $J$ = 8.0 Hz, H-γ of Glu), 1.94 (dq, 1H, dq, $J$ = 14.0, 7.6 Hz, H-β of Glu), 1.79 (dq, 1H, $J$ = 14.8, 7.8 Hz H-β′ of Glu).

$^{13}$C NMR (125 MHz, $D_2O$) $\delta$ (ppm): 177.0 (CO of Glu), 175.7 (γ-CO of Glu), 103.7 (C-1A of CyD), 101.47 (C-1 of CyD), 101.0 (C-1H of CyD), 81.0 (C-4 of CyD), 79.8 (C-4H of CyD), 75.9 (C-5A), 74.0–71.9 (C-3, C-5, C-2 of CyD), 69.7 (C-2AY of CyD), 69.3 (C-2A of CyD), 60.2 (C-6 of CyD), 54.0 (C-α of Glu), 50.9 (C-3A of CyD), 32.2 (C-γ of Glu), 30.2 (C-β of Glu).

The dimer γCyD2Glu was synthesized and purified as reported for βCyD2Glu starting from $\gamma CyDNH_2$. Yield: 34%.

### ESI MS $m/z$ 2703.0 $[M + H]^+$

$^1$H NMR (500 MHz, $D_2O$) $\delta$ (ppm): 5.13–4.97 (m, 12H, H-1 of CyD), 4.94 (d, 1H, $J$ = 4.0 Hz, H-1HX of CyD), 4.92 (d, 1H, $J$ = 4.1 Hz, H-1HY of CyD), 4.90–4.86 (m, 2H, H-1AX, H-1AY of CyD), 4.23 (dd, 1H, $J$ = 8.8, 4.0 Hz, H-3AX of CyD), 4.16 (dd, 1H, $J$ = 9.9, 4.1 Hz, H-3AY CyD), 4.10 (m, 2H, H-5AX, H-5AY CyD), 3.90 (t, 1H, H-4AX of CyD), 3.89–3.69 (m, 63H, H-2AX, H-2AY, H-4AY, H-6AY, H-3, H-5, H-6 of CyD) 3.62–3.47 (m, 28H, H-2, H-4 of CyD), 3.39 (t, 1H, $J$ = 6.5 Hz, H-α of Glu), 2.30 (t, 2H, $J$ = 7.8 Hz, H-γ of Glu), 1.93 (dq, 1H, dq, $J$ = 14.0, 7.6 Hz, H-β of Glu), 1.79 (dq, 1H, $J$ = 14.8, 7.8 Hz H-β′ of Glu).

$^{13}$C NMR (125 MHz, $D_2O$) $\delta$ (ppm): 176.9 (CO of Glu), 175.6 (γ-CO of Glu), 102.9 (C-1A of CD), 101.4 (C-1 of CyD), 101.0 (C-1H of CyD), 80.3 (C-4 of CyD), 79.0 (C-4H of CyD), 75.3 (C-4A), 74.0–71.9 (C-3, C-5, C-2 of CyD), 69.8 (C-2AY of CyD), 69.3 (C-2A of CyD), 60.2 (C-6 of CyD), 54.4 (C-α of Glu), 50.7 (C-3A of CyD), 32.0 (C-γ of Glu), 30.1 (C-β of Glu).

## Ligand and CyD dimers preparation for docking study

The crystal structures of β and γCyDs were extracted from Cambridge Structural Database (https://www.ccdc.cam.ac.uk)[38]

 

with refcode ARUXIU for the βCyD and CYDXPL for the γCyD, respectively. To obtain β- and γ-CyD2Glu dimers, two monomer units were covalently linked in a head-to-head conformation through glutamic acid as the linker using Discovery Studio Visualizer v21.1.0.20298 (**https://www.3ds.com**). The 3D structure of cholesterol was taken from CSD with refcode CHOLME03. Cholate and doxorubicin 3D structures were obtained from Protein Data Bank with PDB code 4n16 and 6kn4, respectively (**https://www.rcsb.org**). Geometry optimization of all structures was carried out using Dreiding-like force field by Biovia Discovery Studio Visualizer v21.1.0.20298.

### Docking calculations

Molecular docking was performed by AutoDock Vina v1.2.0 (The Molecular Graphic Laboratory, The Scripps Research Institute, La Jolla, CA, USA)[39] using cyclodextrin dimers as receptor and cholate, cholesterol and doxorubicin as ligand. Before performing docking calculations, molecules were prepared by AutoDock Tools Tools v1.5.7[38] for what concerns adding polar hydrogen atoms and Gasteiger charges, as well as defining rotatable bonds. Docking analysis was applied to the center of the binding cavity using the following Cartesian coordinates: $x = 14\,551$; $y = 4.012$; $z = -1.152$ with a size of $40 \times 40 \times 40$ for β- and $x = 1176$; $y = 24\,126$; $z = 8115$ with a size of $40 \times 40 \times 40$ for γ-CyD2Glu dimers, respectively. Nine poses (docking output) were generated for each ligand into each model and then ranked by docking score. Complexes obtained were analyzed to find the best solution from both geometrical and energetic points of view. The same procedure was applied for docking with native β and γCyD.

## Conclusions

Here we report the synthesis and characterization of two novel β and γ-cyclodextrin dimers linked by glutamic acid. The dimers were investigated through a multi-technical approach to compare their complexation behavior for doxorubicin or bile acids (cholesterol and cholic acid). Docking experiments showed that β and γ-cyclodextrin dimers form more stable inclusion complexes with a higher degree of binding in comparison to native β and γ-cyclodextrins.

We supported this data by isothermal calorimetry in the case of cholic acid at physiologic pH (cholate species). We found that the binding processes involve two distinct binding modes.

All the inclusion phenomena are both enthalpy and entropy driven with a major contribution of hydrophobic effects, particularly for γ-derivative. As a remarkable novelty, we evidenced that, besides the spacer length and flexibility, the covalent bonding of two cyclodextrins *via* the secondary rim plays a key role in establishing their binding modes and complexation behavior. By comparing thermodynamic parameters, we found that new cyclodextrin dimers showed a 1 : 1 cooperative binding at low (ranging from 0 to 1.5) guest/host molar ratio, whereas at high cholate concentrations, the dimers can include two guest molecules involving both the two cavities. The γ-dimers showed the highest affinity for cholate in 2 : 1 (cholate/dimer) stoichiometry. This result can be of interest for the application of cyclodextrins as nanotherapeutics for the removal of bile acids.

These results may help to provide a blueprint in designing more effective cyclodextrin dimers involving a cooperative binding mode.

## Conflicts of interest

There are no conflicts to declare.

## Acknowledgements

The authors acknowledge support from the Italian Ministero dell'Università e della Ricerca (PON03PE_00216_1).

## Notes and references

1 P. Jansook, N. Ogawa and T. Loftsson, *Int. J. Pharm.*, 2018, **535**, 272–284.
2 G. Crini, S. Fourmentin, É. Fenyvesi, G. Torri, M. Fourmentin and N. Morin-Crini, *Environ. Chem. Lett.*, 2018, **16**, 1361–1375.
3 A. Matencio, G. Hoti, Y. K. Monfared, A. Rezayat, A. R. Pedrazzo, F. Caldera and F. Trotta, *Polymers*, 2021, **13**, 1684.
4 P. F. Garrido, M. Calvelo, A. Blanco-González, U. Veleiro, F. Suárez, D. Conde, A. Cabezón, Á. Piñeiro and R. Garcia-Fandino, *Int. J. Pharm.*, 2020, **588**, 119689.
5 B. Tian, Y. Liu and J. Liu, *Carbohydr. Polym.*, 2020, **242**, 116401.
6 P. Saokham, C. Muankaew, P. Jansook and T. Loftsson, *Molecules*, 2018, 23.
7 O. Swiech, A. Mieczkowska, K. Chmurski and R. Bilewicz, *J. Phys. Chem. B*, 2012, **116**, 1765–1771.
8 X. Song, Y. Wen, J. Ling Zhu, F. Zhao, Z. X. Zhang and J. Li, *Biomacromolecules*, 2016, **17**, 3957–3963.
9 J. Fedoce Lopes, D. Boczar and K. Michalska, *Pharmaceutics*, 2022, **14**, 1389.
10 S. Yi, R. Liao, W. Zhao, Y. Huang and Y. He, *Theranostics*, 2022, **12**, 2560–2579.
11 Y. Yuan, T. Nie, Y. Fang, X. You, H. Huang and J. Wu, *J. Mater. Chem. B*, 2022, **10**, 2077–2096.
12 Z. Liu and Y. Liu, *Chem. Soc. Rev.*, 2022, **51**, 4786–4827.
13 S. T. Jones, V. Cagno, M. Janeček, D. Ortiz, N. Gasilova, J. Piret, M. Gasbarri, D. A. Constant, Y. Han, L. Vuković, P. Král, L. Kaiser, S. Huang, S. Constant, K. Kirkegaard, G. Boivin, F. Stellacci and C. Tapparel, *Sci. Adv.*, 2020, **6**, eaax9318.
14 R. Liao, P. Lv, Q. Wang, J. Zheng, B. Feng and B. Yang, *Biomater. Sci.*, 2017, **5**, 1736–1745.
15 R. Panebianco, M. Viale, N. Bertola, F. Bellia and G. Vecchio, *Dalton Trans.*, 2022, **51**, 5000–5003.
16 M. Řezanka, *Environ. Chem. Lett.*, 2018, **17**, 49–63.
17 D. M. George, R. J. Huntley, K. Cusack, D. B. Duignan, M. Hoemann, J. Loud, R. Mario, T. Melim, K. Mullen, G. Somal, L. Wang and J. J. Edmunds, *PLoS One*, 2018, **13**, e0203567.

18 H. M. Chu, R. X. Zhang, Q. Huang, C. Cai Bai and Z. Z. Wang, *J. Inclusion Phenom. Macrocyclic Chem.*, 2017, **89**, 29–38.
19 M. Naguib, *Anesth. Analg.*, 2007, **104**, 575–581.
20 E. A. Ottinger, N. Carrillo-Carrasco, X. Xu, J. Cradock, P. Terse, S. J. Dehdashti, J. Marugan, W. Zheng, J. C. Mckew, M. L. Kao, I. Scott, S. A. Silber, N. Yanjanin, R. K. Shankar, F. D. Porter, M. Janssen, M. Brewster, L. Portilla, A. Hubbs, W. J. Pavan, J. Heiss, C. H. Vite, S. U. Walkley, D. S. Ory and C. P. Austin, *Curr. Top. Med. Chem.*, 2014, **14**, 330–339.
21 P. F. Garrido, M. Calvelo, A. Blanco-González, U. Veleiro, F. Suárez, D. Conde, A. Cabezón, Á. Piñeiro and R. Garcia-Fandino, *Int. J. Pharm.*, 2020, **588**, 119689.
22 M. Viale, G. Vecchio, I. Maric, M. Cilli, A. Aprile, M. Ponzoni, V. Fontana, E. C. Priori, V. Bertone and M. Rocco, *Toxicol. Appl. Pharmacol.*, 2019, **385**, 114811.
23 N. Bognanni, M. Viale, A. Distefano, R. Tosto, N. Bertola, F. Loiacono, M. Ponassi, D. Spinelli, G. Pappalardo and G. Vecchio, *Molecules*, 2021, **26**, 6046.
24 S. Hong, Z. Li, C. Li, C. Dong and S. Shuang, *Appl. Surf. Sci.*, 2018, **427**, 1189–1198.
25 T. Yamanoi, Y. Oda, K. Katsuraya, T. Inazu and K. Hattori, *Bioorg. Med. Chem.*, 2016, **24**, 635–642.
26 C. Blaszkiewicz, H. Bricout, E. Léonard, C. Len, D. Landy, C. Cézard, F. Djedaíni-Pilard, E. Monflier and S. Tilloy, *Chem. Commun.*, 2013, **49**, 6989–6991.
27 K. Chmurski, P. Stepniak and J. Jurczak, *Carbohydr. Polym.*, 2016, **138**, 8–15.
28 H. Kitagishi, S. Kurosawa and K. Kano, *Chem. – Asian J.*, 2016, **11**, 3213–3219.
29 H. L. McTernan, H. T. Ngo, D. T. Pham, P. Clements, S. F. Lincoln, J. Wang, X. Guo and C. J. Easton, *ChemistrySelect*, 2017, **2**, 1421–1430.
30 I. Kritskiy, R. Kumeev, T. Volkova, D. Shipilov, N. Kutyasheva, M. Grachev and I. Terekhova, *New J. Chem.*, 2018, **42**, 14559–14567.
31 S. Chaudhuri, M. Verderame, T. L. Mako, Y. M. N. D. Y. Bandara, A. I. Fernando and M. Levine, *Eur. J. Org. Chem.*, 2018, 1964–1974.
32 Y. Liu, L. Li, Y. Chen, L. Yu, Z. Fan and F. Ding, *J. Phys. Chem. B*, 2005, **109**, 4129–4134.
33 A. M. Anderson, T. Kirtadze, M. Malanga, D. Dinh, C. Barnes, A. Campo, D. M. Clemens, R. Garcia-Fandiño, Á. Piñeiro and M. S. O'Connor, *Int. J. Pharm.*, 2021, **606**, 120522.
34 S. Shityakov, J. Broscheit and C. Förster, *Int. J. Nanomed.*, 2012, **7**, 3211–3219.
35 P. Bonnet, C. Jaime and L. Morin-Allory, *J. Org. Chem.*, 2001, **66**, 689–692.
36 N. A. Todorova and F. P. Schwarz, *J. Chem. Thermodyn.*, 2007, **39**, 1038–1048.
37 M. F. Sanner, *Structure*, 2005, **13**, 447–462.
38 M. F. Sanner, *J. Mol. Graphics Modell.*, 1999, **17**, 57–61.
39 T. Li, R. Guo, Q. Zong and G. Ling, *Carbohydr. Polym.*, 2022, **276**, 118644.

 